Appendix
Coil Measurements

This appendix digs into methods and instruments by which coil properties can be measured. Single coil measurements provide values for self-inductance, equivalent series resistance and self-resonance frequency. Measurement of coupled coils yields quantitative data on the magnetic coupling and, though usually not desirable, the capacitive coupling that exists between both measurement ports.

A.1 Single Coil Characterisation

A.1.1 General Considerations

Since only the frequency range below self-resonance is relevant for coils that are used in inductive links, an RLC equivalent network is used to model them (see Sect. 2.4 on page 21). The task of characterising a given coil then comes down to identifying the parameters L, R and C in Fig. A.1. Note that only R is assumed to be frequency dependent, while L and C are constants.

The impedance Z of the equivalent RLC network is:

$$Z(s) = \left(sC + \frac{1}{sL + R}\right)^{-1} \tag{A.1}$$

$$= \frac{R + sL}{1 + sCR + s^2LC} \tag{A.2}$$

which exhibits a negative zero at $\omega_z = \frac{R}{L}$, marking the transition from resistive to inductive impedance, and a double pole at the resonance frequency $\omega_0 = \frac{1}{\sqrt{LC}}$. It is implicitly assumed that the damping factor $\zeta = \frac{\omega_0 CR}{2} = \frac{1}{2Q}$ is smaller than one. If this is not the case, the complex conjugate poles split up into two real poles.

If the RLC network is replaced by an RL model, as indicated in Fig. A.1, the influence of capacitance C can be accounted for by use of effective L' and R' values that are frequency dependent (Eqs. (4.51) and (4.52) on page 103). Figure A.2 plots the effective L' and R' values of an RLC tank with $L = 120$ µH, $R = 100$ Ω and $C = 100$ pF. When measuring the inductance and ESR of a coil directly, it will usually be the effective L' and R' values that are returned. If the influence of C is not negligible at the measurement frequency and ω_0 is known, following corrective equations can be applied to derive L and R from the measured L' and R' values:

$$L \approx L'\left[1 - \left(\frac{\omega}{\omega_0}\right)^2\right] \tag{A.3}$$

B. Lenaerts, R. Puers, *Omnidirectional Inductive Powering for Biomedical Implants*,

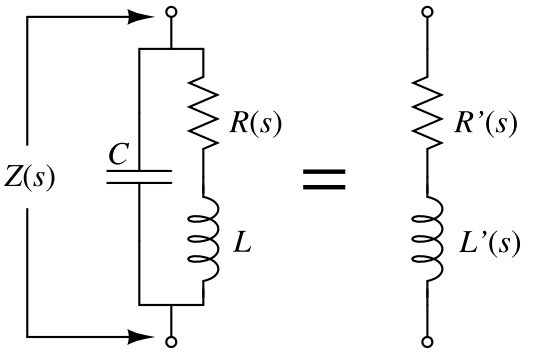

Fig. A.1 Impedance $Z(s)$ of an RLC tank and its equivalent RL network

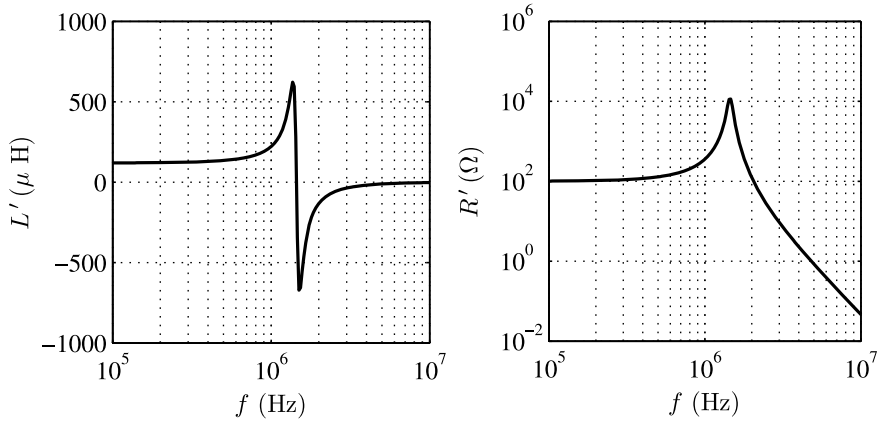

Fig. A.2 Effective inductance L' and effective series resistance R' vs. frequency f of an RLC tank consisting of components $L = 120$ μH, $R = 100\ \Omega$ and $C = 100$ pF

$$R \approx R' \left[1 - \left(\frac{\omega}{\omega_0} \right)^2 \right]^2 \tag{A.4}$$

These equations are the approximate inversions of Eqs. (4.51) and (4.52) on page 103. They are valid only well below ω_0 and for $\omega L \gg R$.

A.1.1.1 Self-inductance

Since the self-inductance L is assumed frequency independent, measurement of L can in principle be done at any point in frequency. For an optimal accuracy however, two arguments should be taken into consideration when selecting the measurement frequency ω:

1. The influence of the inter-winding capacitance should be minimal, so $\omega \ll \omega_0$.
2. The impedance Z should be mainly inductive, hence $\omega \gg \omega_z$.

A.1.1.2 Self-resonance

Neglecting R in the numerator of (A.2), the impedance Z is real at ω_0. The self-resonance frequency $f_0 = \frac{\omega_0}{2\pi}$ is hence measured as the frequency where the impedance's phase crosses zero. From L and ω_0, the inter-winding capacitance C of the equivalent RLC network (Fig. A.1) can be calculated.

For measuring self-resonance, it is imperative that the employed method does not add parasitic capacitance to the coil and as such affects ω_0. The capacitance posed by a coaxial cable for instance will in most practical cases not be negligible against the inter-winding capacitance. It's influence on the measurement result can hence be substantial.

A.1.1.3 Equivalent Series Resistance

The equivalent series resistance (ESR) R of a coil is dependent on frequency. It is therefore to be measured at the frequency of interest.

The large reactance of a coil compromises an accurate measurement of the small ESR in series. For coils with a high quality factor, it is therefore advisable to cancel out the inductive part of the impedance with a high-quality capacitor. By adding the right amount of capacitance to C in Fig. A.1, a tank is formed that is resonant at the frequency of interest. As stated in Sect. A.1.1.2, the impedance Z of an RLC tank is purely resistive at resonance. The value of $Z(s)$ at $s = j\omega_0$ is, still neglecting R in the numerator of Eq. (A.2):

$$Z(j\omega_0) \approx \frac{\omega_0^2 L^2}{R} \tag{A.5}$$

The series resistance R can be hence be found through measurement of $Z(j\omega_0)$.

Apart from the height, also the exact frequency at which the peak occurs in the impedance magnitude $|Z|$ is determined by the damping factor $\zeta = \frac{1}{2Q}$. For a low enough ζ, or a high enough Q, the position of the peak approximately coincides with the pole frequency ω_0 [156]. The height of the peak in $|Z|$ is in that case given by expression (A.5).

A.1.2 One-Port S_{11} Measurement

A vector network analyser (VNA) equipped with an S-parameter test set may be used to characterise the impedance Z_x of a given two-terminal device. Presuming adequate calibration,[1] S-parameters can be measured within a typical accuracy of about 1% [1]. The covered frequency range is from 300 kHz onwards [2].

[1]Calibration is required each time the measurement set-up or an instrument setting has been altered. When measuring over a longer period of time, recalibration may be necessary to account for changes in operation temperature.

A one-port measurement yields the S_{11} reflection coefficient versus frequency. The impedance Z_x of the device under test is calculated from the S_{11} measurement as follows:

$$Z_x = Z_0 \frac{1 + S_{11}}{1 - S_{11}} \tag{A.6}$$

where Z_0 is the characteristic impedance of the instrument and the cabling (usually 50 Ω). In view of Eq. (A.6), it is clear that Z_x is the least susceptible to inaccuracies on S_{11} when it is close to Z_0. For reflection coefficients approaching 1 or -1, which occur at a very high or a very low impedance Z_x respectively, Z_x becomes extremely sensitive to S_{11}. The least inaccuracy on S_{11} then becomes problematic in the calculation of Z_x. Impedance measurement through S_{11} provides an acceptable accuracy on Z_x, of about 10%, within a typical impedance range of 2 Ω to 1.5 kΩ [2].

Self-inductance. Values for L' may be derived from the Z_x values calculated with Eq. (A.6). Next to the general arguments given in Sect. A.1.1.1, the specific method of S-parameter measurement additionally requires $|Z|$ and Z_0 to be of the same order of magnitude for a good accuracy.

Self-resonance. A particular virtue of the S-parameter test is that only the part behind the cable is actually measured. Because the coaxial cabling makes out an intrinsic part of the measurement instrument, it does not affect the impedance of the device under test. This method is hence well suited for determining the self-resonance frequency ω_0 of a coil. It is also useful for manually tuning a given LC tank to a specific resonance frequency, as is normally required in the development of a well performing inductive link (see Sect. 7.3 on page 156).

Equivalent series resistance. A VNA with S-parameter test set can be used to evaluate the impedance magnitude at resonance $|Z(j\omega_0)|$ of an RLC network. The equivalent series resistance R at ω_0 is derived from $|Z(j\omega_0)|$ through Eq. (A.5).

Figure A.3 shows the Z vs. f graph resulting from measurement of the solenoid in Fig. 4.18 on page 113. The high-quality coil is tuned into resonance with even higher-quality NPO capacitors at the frequency of interest, which is about 1055 kHz. Despite long averaging times, a significant degree of error persists around the resonance peak in Fig. A.3, making it hard to determine its precise height. As explained above, this is due to the inherent accuracy limitation of the S_{11} method for very large and very small impedances.

A.1.3 Two-Port Q' Measurement

The method described here can be used to measure the quality factor Q' of a coil, from which its equivalent series resistance R' can be derived.

The measurement set-up is shown in Fig. A.4. As suggested in Sect. A.1.1.3, a high-quality resonance capacitor is employed to cancel out the inductive part of the coil's impedance. A vector network analyser (VNA) provides an oscillation voltage

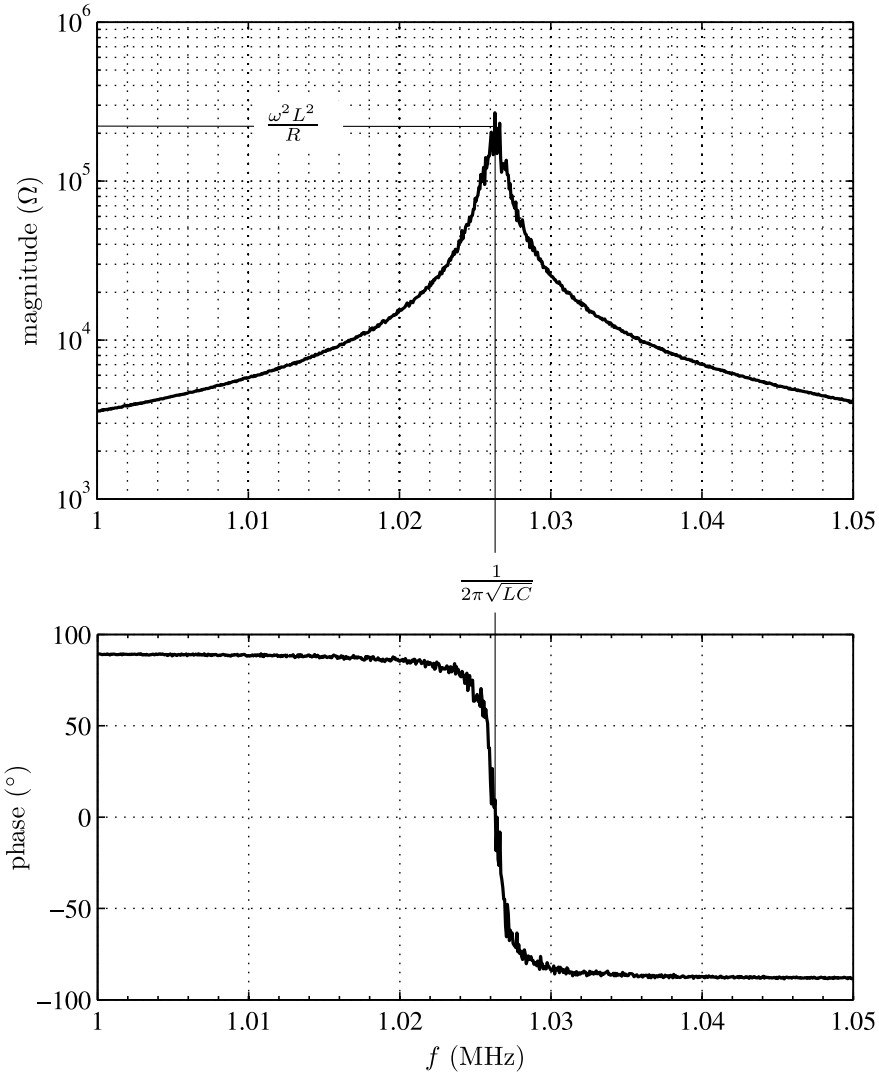

Fig. A.3 Impedance Z vs. frequency f of a high-quality RLC tank around resonance, obtained from S_{11} measurement

and input ports V_1 and V_2, sensing voltages V_1 and V_2 respectively. At resonance frequency ω_0', the impedance constituted by L' cancels out with the variable capacitance and the quality factor Q' is found as the gain in voltage:

$$Q'\left(\omega_0'\right) = \frac{\omega_0' L'\left(\omega_0'\right)}{R'\left(\omega_0'\right)} = \frac{|V_2|}{|V_1|}\left(\omega_0'\right) \tag{A.7}$$

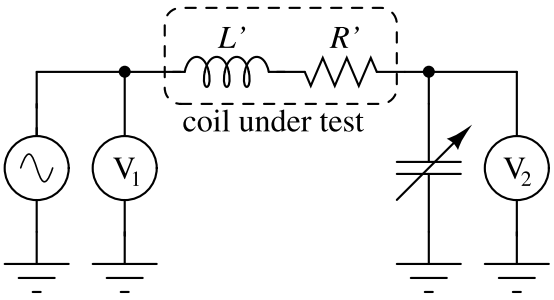

Fig. A.4 Two-port VNA measurement for determining R'

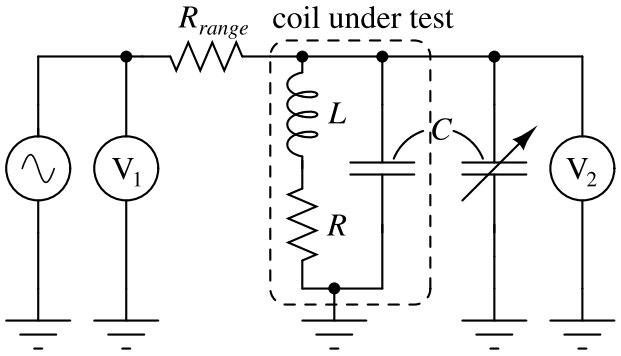

Fig. A.5 Two-port VNA measurement for determining $Z(j\omega_0)$

The measurement can be conducted at different frequencies by changing/adjusting the resonance capacitor and consequently ω_0'. It is clear that the input capacitance of port V_2 and its connection cable makes out part of the resonance capacitor.

Equation (A.4) may be required to distill a value for R out of the measured R' value. Equation (4.51) can be used to calculate L' if found appropriate.

The main demerit of this method is that one of the measurement ports is connected in series with the resonant tank. The added series resistance posed by connection cables and contact resistances compromises the measurement of very low R' values.

The set-up shown in Fig. A.5 avoids breaking up the resonant tank and as such eliminates the influence of series resistances of connection cables. It is now the impedance $|Z(j\omega_0)|$ of the resonant tank, as given by Eq. (A.5), that is evaluated. Note that, since the variable capacitance is added in parallel with the inter-winding capacitance, no R' to R conversion is required. Nevertheless, this method has some drawbacks as well:

1. A very well specified resistor R_{range} is required.
2. For very high resonant impedances $Z(j\omega_0)$, the input resistance of the VNA and the parallel resistance of the coaxial connection cable may become of significance to the damping factor of the RLC network.

A.1.4 Impedance Analysers and LCR Meters

Impedance analysers and LCR meters are specialised instruments for determining the impedance of generic components. Though in principle synonyms, the term impedance analyser is normally reserved for high-end machines with higher frequency ranges (up to 110 MHz) and accuracies while the term LCR meter is used for their lower-end counterparts. Impedance analysers always offer frequency sweeping while LCR meters may be limited to measurement at discrete, prespecified points in frequency.

Though other methods may be encountered,[2] impedance analysers and LCR meters are usually based on the auto balancing bridge method, schematically depicted in Fig. A.6. An operational amplifier and resistor R_{range} convert the current through Z_x to a voltage. Since the operational amplifier limits the attainable frequency and accuracy, higher-end models employ much more sophisticated circuits for the current to voltage conversion [2]. Irrespective of the internal circuitry, four connectors Hc (high current), Hp (high potential), Lc (low current) and Lp (low potential), all referred to the instrument's ground (which in some cases may differ from the chassis's potential), are left for the user to connect to Z_x. The use of long connection cables may affect the measurement results, especially at higher frequencies. Calibrating for a certain set-up helps to diminish this influence. The series inductance due to the connection cabling can be greatly reduced by minimising the area of the current loop I_x through Z_x (Fig. A.6). This is achieved by interconnecting the grounds (or guards) of the Hc and Lc signal lines close to Z_x.

Self-inductance. An impedance analyser or LCR meter offers the most convenient way for measuring the effective inductance L' of a coil. Keeping in mind

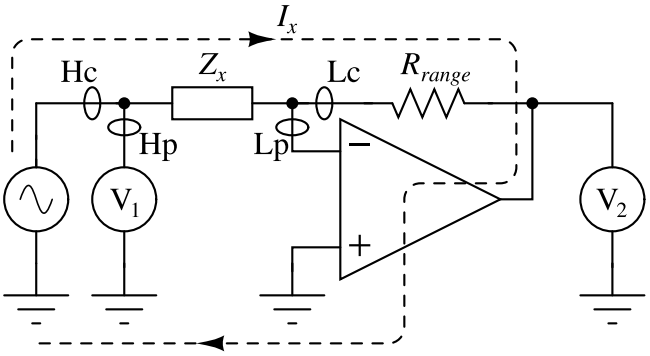

Fig. A.6 The auto balancing bridge method for measuring impedance Z_x

[2]Some impedance analysers are based on the RF I-V method. This allows them to attain much higher frequencies, but limits their impedance range. Still, the RF I-V method reaches higher accuracies and broader impedance ranges then the S-parameter test does and as such is especially suitable for the characterisation of RF components [2].

the general considerations listed in Sect. A.1.1.1, a relatively low measurement frequency will normally be required. The most basic LCR meter will in most cases hence be an adequate instrument for accurately measuring L'.

Self-resonance frequency. An inherent property of the auto balancing bridge method is that it does not add capacitance in parallel with the device under test. It is hence suitable for determining the self-resonance frequency ω_0 of a coil or resonant tank. An impedance analyser or LCR meter that allows frequency sweeping obviously is required. Additional series impedance due to connection cabling scarcely influences the measured ω_0 value, as long as this impedance is negligible to that of the resonant tank.

Equivalent series resistance. Since the accuracy that can be achieved with the auto balancing bridge method is outstanding, it is possible to measure R' together with L' (Fig. A.1). Of course, the measurement should be performed at the frequency of interest and the appliance of Eq. (A.4) hence may be appropriate to derive a meaningful value for R.

For high quality factors (> 25) or small R' values, the use of a high-quality tuning capacitor as suggested in Sect. A.1.1.3 remains advisable. In Fig. A.7, the impedance Z of a high-quality RLC tank is measured vs. frequency. It is the same tank as the one investigated in Fig. A.3. The coil under test hence is again the solenoid in Fig. 4.18 on page 113. The peak height at resonance can now be accurately determined, in contrast with the results obtained from the S_{11} measurement in Fig. A.3. The fact that the resonance frequency itself is different in both measurements, is to blame on a slightly different configuration of the coil's terminal wires. It is instructive to see that if the frequency resolution is inadequate, the peak appears blunted. The actual tank impedance is then larger than would be estimated from the peak height.

A.2 Coupling Characterisation

The purpose of measuring a pair of inductively coupled coils will normally be to retrieve the degree of coupling, i.e. the coupling coefficient k or, equivalently, the single-turn equivalent mutual inductance M_0. One should be aware however that also another coupling mechanism, i.e. capacitive coupling, may contribute to the measurement results. In order to distill a correct value for M_0 out of given measurement data, it is helpful to understand the mechanism behind this capacitive contribution.

The transfer function $\frac{V_1}{V_2}$ of the voltage across the primary coil to the voltage across the secondary coil is obtained through a two-port measurement with a vector network analyser (VNA). Figure A.8 depicts the corresponding, simplified equivalent circuit. Capacitor C_2 accounts for the inter-winding capacitance of the secondary coil and for any other capacitance connected in parallel, like the coaxial cable's capacitance and the VNA's input capacitance. The capacitance in parallel with L_1 has no impact on $\frac{V_1}{V_2}$ as long as voltage drops over the connection cable to port V_1 can be neglected. The omission of the CCVS at the primary side is justified

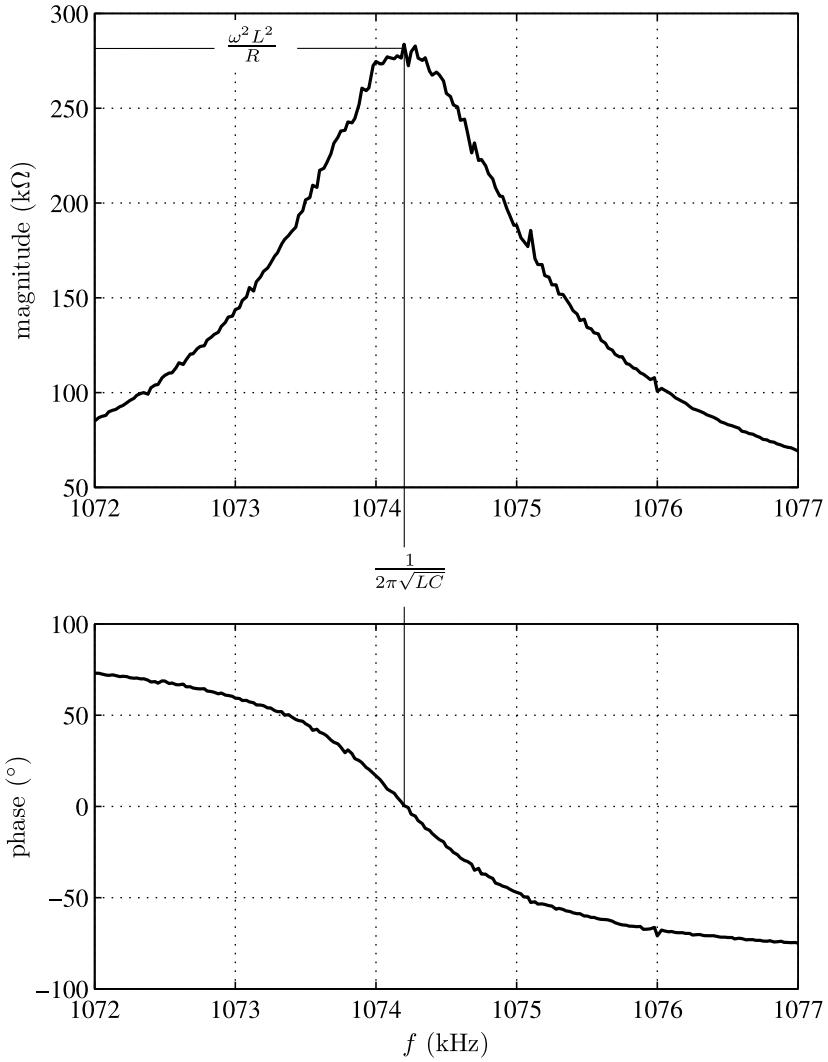

Fig. A.7 Impedance Z vs. frequency of a high-quality RLC tank, measured with an impedance analyser (auto balancing bridge method) around the tank's resonance frequency

in case of loose coupling, or in case no current is flowing though the secondary coil (see Sect. 3.2 on page 53). The capacitive coupling between both coils is modelled through C_p. Capacitive coupling has not been considered thus far because the secondary side was assumed to be left floating. It is only by connecting one of the secondary coil terminals to ground, that an asymmetry in the capacitance distribution is created, opening up the way for capacitive power transmission. From a certain frequency onwards, the capacitive coupling becomes dominant over the inductive coupling, as is shown below.

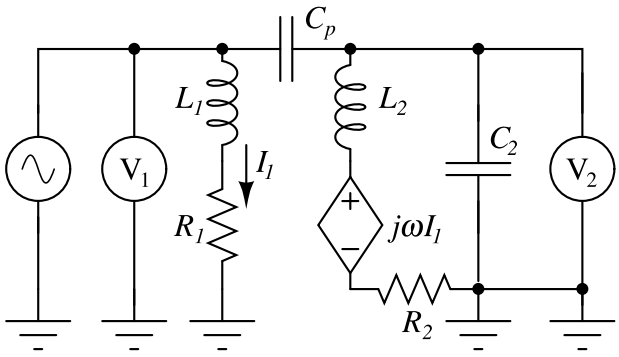

Fig. A.8 Simplified, equivalent schematic of two coupled coils, connected to a vector network analyser for determining the transfer function $\frac{V_1}{V_2}$

From the equivalent network in Fig. A.8, the occurrence of different poles and zeros in $\frac{V_1}{V_2}$ can be predicted. It is assumed that C_p is small and that its contribution to V_2 is negligible at lower frequencies. In that case there is a zero in $\frac{V_1}{V_2}$ at $f_{z1} = 0$, and a pole at f_{p1}, where the primary coil's reactance becomes equal to its series resistance:

$$f_{z1} = 0 \tag{A.8}$$

$$f_{p1} = \frac{R_1}{2\pi L_1} \tag{A.9}$$

A double pole is found at the resonance frequency f_{p2} of the secondary tank:

$$f_{p2} = \frac{1}{2\pi\sqrt{L_2 C_2}} \tag{A.10}$$

In case of strong coupling, f_{p2} may differ slightly from Eq. (A.10) because of Z_{eq} seen in series with the primary coil (Fig. 3.2 on page 44).

It is clear from schematic A.8 that the contribution of C_p to $\frac{V_1}{V_2}$ becomes noticeable only at higher frequencies. In order to determine the cross-over frequency from inductive to capacitive coupling, the secondary coil voltage V_2 is split up into an inductive component V_{2i} and a capacitive component V_{2c}:

$$V_2 = V_{2i} + V_{2c} \tag{A.11}$$

At low frequencies, but beyond f_{p1}, the relationship of V_{2i} and V_{2c} to V_1 can be written as:

$$\frac{V_{2i}}{V_1} \approx j\omega M \frac{1}{j\omega L_1} = \frac{M}{L_1} \tag{A.12}$$

$$\frac{V_{2c}}{V_1} \approx \frac{j\omega L_2}{\frac{1}{j\omega C_p}} = -\omega^2 L_2 C_p \tag{A.13}$$

At the secondary resonance frequency f_{p2}, the impedances of L_2 and C_2 cancel out. The impedance seen over the secondary tank is then given by Eq. (A.5), but is still assumed to be much smaller than the impedance constituted by C_p:

$$\frac{V_{2i}}{V_1} \approx j\omega M \frac{1}{j\omega L_1} \frac{1}{R_2} (-j\omega L_2) = -jQ_2 \frac{M}{L_1} \tag{A.14}$$

$$\frac{V_{2c}}{V_1} \approx \frac{\frac{\omega^2 L_2^2}{R_2}}{\frac{1}{j\omega C_p}} = jQ_2 \omega^2 L_2 C_p \tag{A.15}$$

At frequencies beyond f_{p2}, the impedance of L_2 is dominant over that of C_2 and:

$$\frac{V_{2i}}{V_1} \approx j\omega M \frac{1}{j\omega L_1} \frac{\frac{1}{j\omega C_2}}{j\omega L_2} = -\frac{M}{L_1} \frac{1}{\omega^2 L_2 C_2} \tag{A.16}$$

$$\frac{V_{2c}}{V_1} \approx \frac{C_p}{C_2} \tag{A.17}$$

By comparing Eqs. (A.12)–(A.17), it is seen that the ratio of the capacitive contribution V_{2c} to the inductive contribution V_{2i} is the same for all regions in the transfer function $\frac{V_1}{V_2}$. Relative to V_{2i}, V_{2c} grows quadratically with frequency. Both contributions are equal in magnitude at the cross-over frequency f_{z2}:

$$f_{z2} = \frac{1}{2\pi} \sqrt{\frac{M}{L_1 L_2 C_p}} \tag{A.18}$$

At frequencies beyond f_{z2}, the capacitive coupling becomes dominant over the inductive coupling. The double zero at f_{z2} can consist out of two real zeros (one positive, one negative), or out of two purely imaginary zeros (one positive, one negative), depending on the polarity of the CCVS in schematic A.8. For a positive M in Eqs. (A.12)–(A.17), the inductive and capacitive contributions have a different sign and the zeros are imaginary. This means that at f_{z2}, V_2 in principle becomes zero and a deep, negative peak is observed in the transfer function $\frac{V_1}{V_2}$, together with a phase shift of 180°. The TF that is measured in this situation is plotted in solid grey in Fig. A.9. The black dashed line plots the transfer function $\frac{V_1}{V_2}$ for the same coil pair, but with a reversed secondary coil orientation. By rotating the secondary coil over 180° around its centre, or by swapping the ground connection at the primary or secondary side, the sign of the inductive contribution V_{2i} is reversed. In that case the zeros at f_{z2} are real and there is no negative peak, nor a phase shift of 180° to be seen in $\frac{V_1}{V_2}$. The intrinsic 180° phase shift is not shown in Fig. A.9 in order to better show the similarity and to highlight to additional phase shift at f_{z2} for one particular orientation.

The influence of the capacitive coupling on $\frac{V_1}{V_2}$ is already noticeable at frequencies below f_{z2}. For the measured example in Fig. A.9 for instance, the height of the peak at secondary resonance is affected by a capacitive contribution. It may also

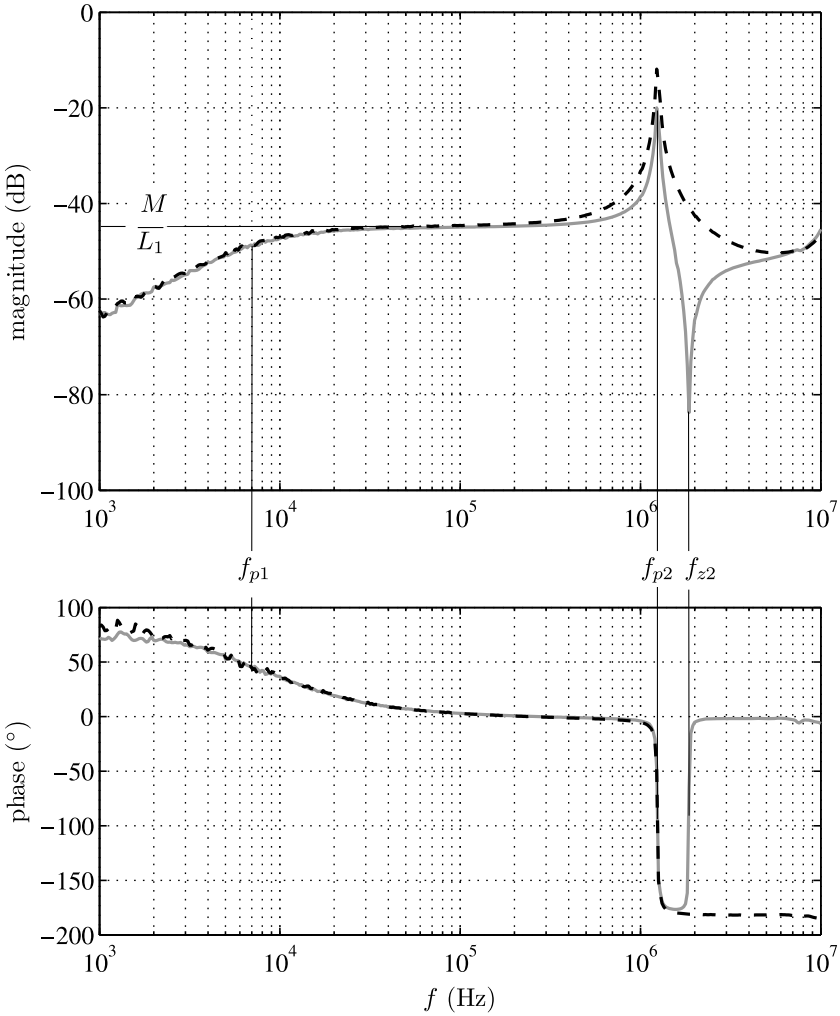

Fig. A.9 Transfer function $\frac{V_1}{V_2}$ measured for two opposite secondary coil orientations. The phase offset of 180° between both orientations has been subtracted out

occur that the cross-over frequency f_{z2} is smaller than the secondary resonance frequency f_{p2}. The expressions (A.10) and (A.18) for f_{p2} and f_{z2} respectively, remain valid in that case.

A good way to eliminate the capacitive contribution, is to measure $\frac{V_1}{V_2}$ for two opposite coil orientations and to subtract the results. Only the inductive part then remains, since its sign changes with the coil orientation, unlike the sign of the capacitive contribution.

For measuring the mutual inductance M, one can restrict oneself to the flat region in the frequency response, well below f_z. One can verify the validity of the obtained

result by reversing the ground connection at either primary or secondary side, or by rotating one of the coils over 180°. For the coil set measured in Fig. A.9, $\frac{M}{L_1} = 5.6 \times 10^{-3}$. Knowing that $L_1 = 56.3$ µH, $N_1 = 13$ and $N_2 = 145$, the single-turn equivalent mutual inductance M_0 is found to be:

$$M_0 = 168 \text{ pH} \tag{A.19}$$

which is in agreement with finite element calculations.

Through Eq. (A.18) and the knowledge of f_{z2} (= 1.86 MHz) and L_2 (= 102.6 µH), also parameter C_p can be determined:

$$C_p = 400 \text{ fF} \tag{A.20}$$

References

1. Agilent Technologies Inc.: Agilent 8753ET/ES, 8753ET and 8753ES Network Analyzers, 30 kHz to 3 or 6 GHz, February 2001
2. Agilent Technologies Inc.: Impedance Measurement Handbook, July 2006
3. Akin, T., Najafi, K., Bradley, R.M.: A wireless implantable multi-channel digital neural recording system for a micromachined sieve electrode. IEEE Journal of Solid-State Circuits **33**, 109–118 (1998)
4. Appleyard, M., Fireman, Z., Glukhovsky, A., Jacob, H., Shreiver, R., Kadirkamanathan, S., Lavy, A., Lewkowicz, S., Scapa, E., Shofti, R., Swain, P., Zaretsky, A.: A randomized trial comparing wireless capsule endoscopy with push enteroscopy for the detection of small-bowel lesions. Gastroenterology **119**(6), 1431–1438 (2000)
5. Archambeault, B.R.: PCB Design for Real-World EMI Control. Kluwer Academic, Dordrecht (2004). ISBN 1-4020-7130-2
6. Arena, A., Boulougoura, M., Chowdrey, H.S., Dario, P., Harendt, C., Irion, K.M., Kodogiannis, V., Lenaerts, B., Menciassi, A., Puers, R., Scherjon, C., Turgis, D.: Intracorporeal videoprobe (IVP). In: Bos, L. et al. (eds.) Medical and Care Compunetics 2, pp. 167–174. IOS Press, Amsterdam (2005). ISBN 978-1-58603-520-4
7. Avonwood Developments Ltd., U.K.: Eureka 311—132 kHz Readers (2004)
8. Avratoglou, C.P., Voulgaris, N.C.: A new method for the analysis and design of the class E power amplifier taking into account the Q_L factor. IEEE Transactions on Circuits and Systems **34**, 687–691 (1987)
9. Avratoglou, C.P., Voulgaris, N.C., Ioannidou, F.I.: Analysis and design of a generalized class E tuned power amplifier. IEEE Transactions on Circuits and Systems **36**, 1068–1079 (1989)
10. Barnes, F.S.: Interaction of DC and ELF electric fields with biological materials and systems. In: Polk, C., Postow, E. (eds.) Handbook of Biological Effects of Electromagnetic Fields, 2nd edn., chap. 2, pp. 103–148. CRC Press, Boca Raton (1996). ISBN 0-8493-0641-8
11. Bell, T.E., Wise, K.D., Anderson, D.J.: A flexible micromachined electrode array for a cochlear prosthesis. Sensors and Actuators, A, Physical **66**, 63–69 (1998)
12. Belmans, R., Hameyer, K.: Elektrische Energie, Fundamenten en Toepassingen. Garant, Leuven (1999). ISBN 90-5350-924-0
13. Bovie, U.S., Aaron 3250™, 2006
14. Bowman, W.C., Magalhaes, F.M., Suiter, W.B., Ziesse, N.G.: Resonant rectifier circuits. US Patent 4 685 041, 1987
15. Burny, F., Donkerwolcke, M., Moulart, F., Bourgois, R., Puers, R., Van Schuylenbergh, K., Barbosa, M., Paiva, O., Rodes, F., Bégueret, J.B., Lawes, P.: Concept, design and fabrication of smart orthopedic implants. Medical Engineering & Physics **22**, 469–479 (2000)
16. Chatterjee, I., Wu, D., Gandhi, O.P.: Human body impedance and threshold currents for perception and pain for contact hazard analysis in the VLF-MF band. IEEE Transactions on Biomedical Engineering **33**, 486–494 (1989)
17. Claes, W., Vandevoorde, G.: Draadloze registratie van de intra-oculaire druk door resonantiedetectie. Master thesis, K.U. Leuven, Belgium (1996)
18. Claes, W., Sansen, W., Puers, R.: A 40 μa/channel compensated 18-channel strain gauge measurement system for stress monitoring in dental implants. IEEE Journal of Solid-State Circuits **37**, 293–301 (2002)
19. COMSOL AB: Comsol Multiphysics Users's Guide, version 3.2, September 2005
20. COMSOL AB: Electromagnetics Module Model Library, version 3.2, September 2005
21. COMSOL AB: Electromagnetics Module User's Guide, version 3.2, September 2005

22. Coosemans, J., Puers, R.: An autonomous bladder pressure monitoring system. Sensors and Actuators A: Physical **123–124**, 155–161 (2005)
23. Coppens, S.: Klasse E versterker met automatische impedantieaanpassing voor inductieve vermogenoverdracht. Master thesis, K.U. Leuven, Belgium (2005)
24. Costamagna, G., Shah, S.K., Riccioni, M.E., Foschia, F., Mutignani, M., Perri, V., Vecchioli, A., Brizi, M.G., Picciocchi, A., Marano, P.: A prospective trial comparing small bowel radiographs and video capsule endoscopy for suspected small bowel disease. Gastroenterology **123**(4), 999–1005 (2002)
25. Dierckx, P., Piessens, R.: Vectorvelden Lijnintegralen en Oppervlakte-integralen. In: Analyse I—Deel 2, chap. 11, pp. 233–253. Vlaamse Technische Kring v.z.w., Leuven (1997)
26. Dimbylow, P.J.: FDTD calculations of the whole-body averaged sar in an anatomically realistic voxel model of the human body from 1 MHz to 1 GHz. Physics in Medicine and Biology **42**, 479–490 (1997)
27. Directive 2004/40/EC of the European parliament and of the council of 29 April 2004, on the minimum health and safety requirements regarding exposure of workers to the risks arising from physical agents (electromagnetic fields) (18th individual directive within the meaning of article 16(1) of directive 89/391/EEC), 2004
28. Donaldson, N. de N.: Voltage regulators for implants powered by coupled coils. Medical and Biological Engineering and Computing **21**, 756–761 (1983)
29. Donaldson, N. de N.: Use of feedback with voltage regulators for implants powered by coupled coils. Medical and Biological Engineering and Computing **23**, 291 (1985)
30. Donaldson, N. de N.: Comments on "efficient transdermal links with coupling-insensitive gain". IEEE Transactions on Biomedical Engineering **35**, 280–280 (1988)
31. Donaldson, N. de N.: Effect of the metallic seal of a hermetic enclosure on the induction of power to an implant. Medical and Biological Engineering and Computing **30**, 63–68 (1992)
32. Donaldson, N. de N., Perkins, T.A.: Analysis of resonant coupled coils in the design of radio frequency transcutaneous links. Medical and Biological Engineering and Computing **21**, 612–627 (1983)
33. Donaldson, P.E.K.: Power for neurological prostheses: a simple r.f. link with improved performance. J. Biomed. Eng. **9**, 194–197 (1987)
34. Donaldson, P.E.K.: Three separation-insensitive radio frequency inductive links. J. Med. Eng. and Technol. **11**, 23–29 (1987)
35. Elliott, R.S.: Electromagnetics: History, Theory, and Applications. IEEE Press, New Jersey (1993)
36. Elmed Inc., U.S.: Elektrotom 600 RFS, 2006
37. Findlay, R.P., Dimbylow, P.J.: FDTD calculations of specific energy absorption rate in a seated voxel model of the human body from 10 MHz to 3 GHz. Physics in Medicine and Biology **51**, 2339–2352 (2006)
38. Finkenzeller, K.: RFID Handbook. Wiley, New York (2003). ISBN 9780470844021
39. Finkenzeller, K.: Physical Principles of RFID Systems. In: RFID Handbook, chap. 4, pp. 62–66. Wiley (2003). ISBN 9780470844021
40. Finkenzeller, K.: Frequency Ranges and Radio Licensing Regulations. In: RFID Handbook, chap. 5, pp. 161–181. Wiley, New York (2003). ISBN 9780470844021
41. Finkenzeller, K.: Coding and Modulation. In: RFID Handbook, chap. 6, pp. 183–194. Wiley, New York (2003). ISBN 9780470844021
42. Fireman, Z., Mahajna, E., Broide, E., Shapiro, M., Fich, L., Sternberg, A., Kopelman, Y., Scapa, E.: Diagnosing small bowel Crohn's disease with wireless capsule endoscopy. Gut **52**, 390–392 (2003)
43. Forde, M., Ridgely, P.: Implantable cardiac pacemakers. In: Bronzino, J.D. (ed.) The Biomedical Engineering Handbook, pp. 1258–1274. CRC Press, Boca Raton (1995). ISBN 0-8493-8346-3
44. Forster, I.C.: Theoretical design and implementation of a transcutaneous, multichannel stimulator for neural prosthesis applications. Journal of Biomedical Engineering **3**(2), 107–120 (1981)

45. Foster, K.R., Schwan, H.P.: Dielectric properties of tissues. In: Polk, C., Postow, E. (eds.) Handbook of Biological Effects of Electromagnetic Fields, 2nd edn., chap. 2, pp. 103–148. CRC Press, Boca Raton (1996). ISBN 0-8493-0641-8
46. Frankel, R.B., Liburdy, R.P.: Biological effects of static magnetic fields. In: Polk, C., Postow, E. (eds.) Handbook of Biological Effects of Electromagnetic Fields, 2nd edn., chap. 3, pp. 149–184. CRC Press, Boca Raton (1996). ISBN 0-8493-0641-8
47. Furman, S., Raddi, W.J., Escher, D.J., Denize, A., Schwedel, J.B., Hurwitt, E.S.: Rechargeable pacemaker for direct myocardial implantation. Archives of Surgery **91**, 796–800 (1965)
48. Gabriel, C., Gabriel, S., Corthout, E.: The dielectric properties of biological tissues: I. Literature survey. Physics in Medicine and Biology **41**, 2231–2249 (1996)
49. Gabriel, S., Lau, R.W., Gabriel, C.: The dielectric properties of biological tissues: II. Measurements in the frequency range 10 Hz to 20 GHz. Physics in Medicine and Biology **41**, 2251–2269 (1996)
50. Galbraith, D.C., Soma, M., White, R.L.: A wide-band efficient inductive transdermal power and data link with coupling insensitive gain. IEEE Transactions on Biomedical Engineering **34**, 265–275 (1987)
51. Gandhi, O.P.: The ANSI radio frequency safety standard: its rationale and some problems. IEEE Eng. Med. Biol. Mag. **6**(11), 22–25 (1987)
52. Gandhi, O.P., Chatterjee, I.: Radio-frequency hazards in the VLF to MF band. Proceedings of the IEEE **70**, 1462–1464 (1982)
53. Geddes, L.A., Roeder, R.A.: De Forest and the first electrosurgical unit. IEEE Engineering in Medicine and Biology Magazine **22**(1), 84–87 (2003)
54. Geselowitz, D.B., Hoang, Q.T.N., Gaumond, R.P.: The effects of metals on a transcutaneous energy transmission system. IEEE Transactions on Biomedical Engineering **39**, 928–934 (1992)
55. Ghovanloo, M., Najafi, K.: Fully integrated power supply design for wireless biomedical implants. In: 2nd Annual International IEEE-EMB Special Topic Conference on Microtechnologies in Medicine & Biology, Madison, U.S., May 2–4, 2002, pp. 414–419. IEEE Press, New York. ISBN 0-7803-7480-0
56. Graetzer, D.: Transductor-regulators for switched-mode power supplies. IEEE Transactions on Magnetics **16**(5), 922–924 (1980)
57. Grevendonck, W.: Algemene Natuurkunde: deel B. Vlaamse Technische Kring v.z.w., Leuven (1997)
58. Grevendonck, W.: Algemene Natuurkunde: deel C, pp. 14.39–14.44. Vlaamse Technische Kring v.z.w., Leuven (1998)
59. Grover, F.W.: Inductance Calculations. Dover Publications, New York (2004)
60. Hamamatsu Photonics, K.K.: Characteristics and use of infrared detectors. Hamamatsu City, Japan (2004)
61. Harrison, R.G.: A nonlinear theory of class C transistor amplifiers and frequency multipliers. IEEE Journal of Solid-State Circuits **2**, 93–102 (1967)
62. Hart, L.W., Ko, H.W., Meyer, J.H. Jr., Vasholz, D.P., Joseph, R.I.: A noninvasive electromagnetic conductivity sensor for biomedical applications. IEEE Transactions on Biomedical Engineering **35**, 1011–1022 (1988)
63. Hoang, Q.T., Hete, B.F., Gaumond, R.P.: Comments on radio-frequency coils in implantable devices: misalignment analysis and design procedure. IEEE Transactions on Biomedical Engineering **40**, 715 (1993)
64. Hochberg, L.R., Serruya, M.D., Friehs, G.M., Mukand, J.A., Saleh, M., Caplan, A.H., Branner, A., Chen, D., Penn, R.D., Donoghue, J.P.: Neuronal ensemble control of prosthetic devices by a human with tetraplegia. Nature **442**, 164–171 (2006)
65. Hochmair, E.S.: System optimization for improved accuracy in transcutaneous signal and power transmission. IEEE Transactions on Biomedical Engineering **31**, 177–186 (1984)
66. Iddan, G., Meron, G., Glukhovsky, A., Swain, P.: Wireless capsule endoscopy. Nature **405**, 417–417 (2000)
67. IEEE standard for safety levels with respect to human exposure to radio frequency electromagnetic fields, 3 kHz to 300 GHz (2006). ISBN 0-7381-4834-2

68. Inan, U.S., Inan, A.S.: Maxwell's Equations and Electromagnetic Waves. In: Electromagnetic Waves, chap. 1, pp. 1–14. Prentice Hall, New Jersey (2000). ISBN 0-201-36179-5
69. Inan, U.S., Inan, A.S.: Plane Waves in Lossy Media. In: Electromagnetic Waves, sect. 2.3, pp. 38–58. Prentice Hall, New Jersey, 2000, ISBN 0-201-36179-5
70. Inan, U.S., Inan, A.S.: Electromagnetic Radiation and Elementary Antennas In: Electromagnetic Waves, sect. 6.5, pp. 476–499. Prentice Hall, New Jersey (2000). ISBN 0-201-36179-5
71. International Agency for Research on Cancer: Non-ionizing radiation, part 1: Static and extremely low-frequency (ELF) electric and magnetic fields. In: IARC Monographs on the Evaluation of Carcinogenic Risks to Humans, vol. 80 (2002)
72. International Commission on Non-Ionizing Radiation Protection: Guidelines for limiting exposure to time-varying electric, magnetic, and electromagnetic fields (up to 300 GHz). Health Physics **74**(4), 494–522 (1998)
73. Intersil: EL7104 High Speed, Single Channel, Power MOSFET Driver, July 2006
74. Kamon, M., Ttsuk, M.J., White, J.K.: FASTHENRY: A multipole-accelerated 3-D inductance extraction program. IEEE Transactions on Microwave Theory and Techniques **42**(9), 1750–1758 (1994)
75. Kanal, E., Gillen, J., Savitz, D.A., Evans, J.A., Shellock, F.G.: Survey of reproductive health among female MR workers. Radiology **187**, 395–399 (1993)
76. Kazimierczuk, M.K.: Class D current-driven rectifiers for resonant DC/DC converter applications. IEEE Transactions on Industrial Electronics **37**, 436–444 (1990)
77. Kazimierczuk, M.K.: Analysis of class E zero-voltage-switching rectifier. IEEE Transactions on Circuits and Systems **37**, 747–755 (1990)
78. Kazimierczuk, M.K., Czarkowski, D.: Resonant Power Converters, part I: Rectifiers, pp. 7–145. Wiley, New York (1995). ISBN 0-471-04706-6
79. Kazimierczuk, M.K., Czarkowski, D.: Resonant Power Converters, part II: Inverters, pp. 149–392. Wiley, New York (1995). ISBN 0-471-04706-6
80. Kazimierczuk, M.K., Józwik, J.: Class E zero-voltage-switching and zero-current-switching rectifiers. IEEE Transactions on Circuits and Systems **37**, 436–444 (1990)
81. Kazimierczuk, M.K., Józwik, J.: Analysis and design of class E zero-current-switching rectifier. IEEE Transactions on Circuits and Systems **37**, 1000–1009 (1990)
82. Kazimierczuk, M.K., Puczko, K.: Class E tuned power amplifier with shunt inductor. IEEE Journal of Solid-State Circuits **16**, 2–7 (1981)
83. Kazimierczuk, M.K., Puczko, K.: Exact analysis of class E tuned power amplifier at any Q and switch duty cycle. IEEE Transactions on Circuits and Systems **34**, 149–159 (1987)
84. Kazimierczuk, M.K., Puczko, K.: Class E tuned power amplifier with antiparallel diode or series diode at switch, with any loaded Q and switch duty cycle. IEEE Transactions on Circuits and Systems **36**, 1201–1209 (1989)
85. Kennelly, A.E., Affel, H.A.: Skin-effect resistance measurements of conductors, at radio-frequencies up to 100,000 cycles per second. Proceedings of the IRE **4**(6), 523–574 (1916)
86. Ko, W.H., Liang, S.P., Fung, C.D.F.: Design of radio-frequency powered coils for implant instruments. Medical and Biological Engineering and Computing **15**, 634–640 (1977)
87. Krauss, H.L., Bostian, C.W., Raab, F.H.: Solid State Radio Engineering. Wiley, New York (1980). ISBN 0-471-03018-X
88. Kwok, M.C., Pepper, M.G.: Noninvasive detection of ventricular wall motion by electromagnetic coupling, part I theory: the changes in the reflected impedance of a coil over a semi-infinite medium with properties ranging from lossy dielectric to a conductor. Medical and Biological Engineering and Computing **29**, 136–140 (1991)
89. La Course, J.R., Miller III, W.T., Vogt, M., Selikowitz, S.M.: Effect of high-frequency current on nerve and muscle tissue. IEEE Transactions on Biomedical Engineering **32**, 82–86 (1985)
90. Lai, Y.M.: Power supplies. In: Rashid, M.H. (ed.) Power Electronics Handbook, chap. 23, pp. 593–618. Academic Press, San Diego (2007). ISBN 0120884798
91. Lammeraner, J., Stafl, M.: Eddy Currents. National Technical Information Service (1966)
92. Lee, Y.: Antenna Circuit Design for RFID Applications, Microchip (2003), application note AN710

93. Lee, Y.-S., Chow, H.L.: Diode rectifiers. In: Rashid, M.H. (ed.) Power Electronics Handbook, chap. 10, pp. 145–178. Academic Press, San Diego (2007). ISBN 0120884798
94. Lenaerts, B., Puers, R.: Inductive powering of a freely moving system. In: Eurosensors XVIII, Rome, Italy, September 12–15, 2004, pp. 484–485
95. Lenaerts, B., Puers, R.: Inductive powering of a freely moving system. Sensors and Actuators A: Physical **123–124**, 522–530 (2005)
96. Lenaerts, B., Puers, R.: An omnidirectional transcutaneous power link for capsule endoscopy. In: International Workshop on Wearable and Implantable Body Sensor Networks, Boston, U.S., April 3–5, 2006, pp. 46–49. ISBN 0-7695-2547-4
97. Lenaerts, B., Puers, R.: An inductive power link for a wireless endoscope. Biosensors and Bioelectronics **22**, 1390–1395 (2007)
98. Lenaerts, B., Puers, R.: Automatic inductance compensation for class E driven flexible coils. Sensors and Actuators A: Physical **145–146**, 154–160 (2008)
99. Lenaerts, B., Peeters, F., Puers, R.: Closed-loop transductor-compensated class E driver for inductive links. In: TRANSDUCERS'07 and Eurosensors XXI, Lyon, France, June 10–14, 2007, vol. 1, pp. 65–68. ISBN 1-4244-0841-5
100. Leroux, P.: Low-noise Amplification in CMOS High-Frequency Receivers. Ph.D. thesis, K.U. Leuven, Belgium (2004)
101. Leuerer, T., Mokwa, W.: Planar coils with magnetic layers for optimized energy transfer in telemetric systems. Sensors and Actuators A: Physical **116**, 410–416 (2004)
102. Mandojana, J.C., Herman, K.J., Zulinski, R.E.: A discrete/continuous time-domain analysis of a generalized class E amplifier. IEEE Transactions on Computer-Aided Design of Integrated Circuits and Systems **37**, 1057–1060 (1990)
103. Massarini, A., Kazimierczuk, M.K.: Self-capacitance of inductors. IEEE Transactions on Power Electronics **12**, 671–676 (1997)
104. Maswood, A.I.: The power diode. In: Rashid, M.H. (ed.) Power Electronics Handbook, chap. 2, pp. 15–26. Academic Press, San Diego (2007). ISBN 0120884798
105. Mattiussi, C.: An analysis of finite volume, finite element, and finite difference methods using some concepts from algebraic topology. Journal of Computational Physics **133**, 289–309 (1997)
106. Mattiussi, C.: The finite volume, finite element, and finite difference methods as numerical methods for physical field problems. http://citeseer.ist.psu.edu/article/mattiussi00finite.html (2000)
107. Maxwell, J.C.: A dynamical theory of the electromagnetic field. Philosophical Transactions of the Royal Society of London **155**, 459–512 (1865)
108. Mentor Graphics: Eldo User's Manual, 2005, Software Version 6.6_1 Release 2005.3
109. Mohan, N., Undeland, T.M., Robbins, W.P.: Power Electronics. Wiley, New York (2003). ISBN 0-471-42908-2
110. New England Wire Technologies, Lisbon, USA: Litz & winding wire (2007)
111. Niknejad, A.M., Meyer, R.G.: Analysis, design and optimization of spiral inductors and transformers for Si RF IC's. IEEE Journal of Solid-State Circuits **33**(10), 1470–1481 (1998)
112. Niknejad, A.M., Meyer, R.G.: Design, Simulation and Applications of Inductors and Transformers for Si RF ICs. Kluwer Academic, Boston (2000)
113. Nitz, W.A., Bowman, W.C., Dickens, F.T., Magalhaes, F.M., Strauss, W., Suiter, W.B., Ziesse, N.G.: A new family of resonant rectifier circuits for high frequency DC-DC converter applications. In: Third Annual IEEE Applied Power Electronics Conference and Exposition, New Orleans, U.S., February 1–5, 1988, pp. 12–22
114. Peeters, F.: Klasse E versterker met automatische impedantieaanpassing voor inductieve vermogenoverdracht. Master thesis, K.U. Leuven, Belgium (2006)
115. Pepper, M.G., Taylor, D.J.E., Kwok, M.C.: Noninvasive detection of ventricular wall motion by electromagnetic coupling, part II experimental: cardiokyomography. Medical and Biological Engineering and Computing **29**, 141–148 (1991)
116. Philips Components: Class 1, NP0 50/100/200/500 V Noble Metal Electrode surface mount ceramic multilayer capacitors, February 1999

117. Polk, C., Postow, E.: Handbook of Biological Effects of Electromagnetic Fields, 2nd edn., pp. 25–102. CRC Press, Boca Raton (1996). ISBN 0-8493-0641-8
118. Press, A.: Resistance and reactance of massed rectangular conductors. Physical Review **8**, 417–422 (1916)
119. Puers, R., Vandevoorde, G.: Recent progress on transcutaneous energy transfer for total artificial heart systems. Artificial Organs **25**, 400–405 (2001)
120. Puers, R., Catrysse, M., Vandevoorde, G., Collier, R., Louridas, E., Burny, F., Donkewolcke, M., Moulart, F.: An implantable system for detecting loosening of a hip prosthesis. In: Eiler, J., Alcorn, D., Neuman, M. (eds.) 15th International Symposium on Biotelemetry, Juneau, Alaska U.S., May 9–14, 1999, pp. 652–660. ISBN 0-9707533-0-6
121. Puers, R., Catrysse, M., Vandevoorde, G., Collier, R.J., Louridas, E., Burny, F., Donkerwolcke, M., Moulart, F.: A telemetry system for the detection of hip prosthesis loosening by vibration analysis. Sensors and Actuators A: Physical **85**, 42–47 (2000)
122. Raab, F.H.: Idealized operation of the class E tuned power amplifier. IEEE Transactions on Circuits and Systems **CAS-24**, 725–735 (1977)
123. Raab, F.H.: Effects of circuit variations on the class E tuned power amplifier. IEEE Journal of Solid-State Circuits **13**, 239–247 (1978)
124. Raab, F.H., Sokal, N.O.: Transistor power losses in the class E tuned power amplifier. IEEE Journal of Solid-State Circuits **13**, 912–914 (1978)
125. Rashid, M.H.: Power Electronics Handbook. Academic Press, San Diego (2007). ISBN 0120884798
126. Ravazzani, P., Ruohonen, J., Tognola, G., Anfosso, F., Ollikainen, M., Ilmoniemi, R.J., Grandori, F.: Frequency-related effects in the optimization of coils for the magnetic stimulation of the nervous system. IEEE Transactions on Power Electronics **49**, 463–471 (2002)
127. Redl, R., Balogh, L.: Power-factor correction in bridge and voltage-doubler rectifier circuits with inductors and capacitors. In: 10th Annual Applied Power Electronics Conference and Exposition, Dallas, U.S., March 5–9, 1995, vol. 1, pp. 466–472. ISBN 0-7803-2482-X
128. Rey, J.-F., Kuznetsov, K., Vazquez-Ballesteros, E.: Olympus capsule endoscope for small and large bowel exploration. Gastrointestinal Endoscopy **63**, AB176 (2006)
129. Reynaert, P.: CMOS Power Amplifiers for Wireless Communication. Ph.D. thesis, K.U. Leuven, Belgium (2006)
130. Reynaert, P., Steyaert, M.S.J.: A 2.45 GHz 0.13 μm CMOS PA with parallel amplification. IEEE Journal of Solid-State Circuits **42**, 551–562 (2007)
131. Reynaert, P., Mertens, K.L.R., Steyaert, M.S.J.: A state-space behavioral model for CMOS class E power amplifiers. IEEE Transactions on Computer-Aided Design of Integrated Circuits and Systems **22**, 132–138 (2003)
132. Rizzo III, J.F., Wyatt, J., Loewenstein, J., Kelly, S., Shire, D.: Perceptual efficacy of electrical stimulation of human retina with a microelectrode array during short-term surgical trials. Investigative Ophthalmology and Visual Science **44**, 5362–5369 (2003)
133. Sacristán, J., Segura, F., Osés, M.T.: Bidirectional telemetry for implantable systems. In: IEEE International Symposium on Circuits and Systems, Island of Kos, Greece, May 21–24, 2006, pp. 349–352
134. Schenck, J.F., Dumoulin, C.L., Redington, R.W., Kresseland, H.Y., Elliott, R.T., McDougall, I.L.: Human exposure to 4.0-Tesla magnetic fields in a whole-body scanner. Medical Physics **19**, 1089–1098 (1992)
135. Schnakenberg, U., Walter, P., vom Bögel, G., Krüger, C., Lüdtke-Handjery, H.C., Richter, H.A., Specht, W., Ruokonen, P., Mokwa, W.: Initial investigations on systems for measuring intraocular pressure. Sensors and Actuators A: Physical **85**, 287–291 (2000)
136. Schnakenberg, U., Krüger, C., Pfeffer, J.-G., Mokwa, W., vom Bögel, G., Günther, R., Schmitz-Rode, T.: Intravascular pressure monitoring system. Sensors and Actuators A: Physical **110**, 61–67 (2004)
137. Schuder, J.C., Gold, J.H., Stoeckle, H., Holland, J.A.: The relationship between the electric field in a semi-infinite conductive region and the power input to a circular coil on or above the surface. Medical and Biological Engineering and Computing **15**, 227–233 (1976)

138. Schwarz, M., Ewe, L., Hauschild, R., Hosticka, B.J., Huppertz, J., Kolnsberg, S., Mokwa, W., Trieu, H.K.: Single chip CMOS imagers and flexible microelectronic stimulators for a retina implant system. Sensors and Actuators A: Physical **83**, 40–46 (2000)
139. Silver, A.W., Root, G., Byron, F.X., Sandberg, H.: Externally rechargeable cardiac pacemaker. The Annals of Thoracic Surgery **92**, 380–388 (1965)
140. Smith, D.R., Pendry, J.B., Wiltshire, M.C.K.: Metamaterials and negative refractive index. Science **305**, 788–792 (2004)
141. Sokal, N.O., Raab, F.H.: Harmonic output of class-E RF power amplifiers and load coupling network design. IEEE Journal of Solid-State Circuits **12**, 86–88 (1977)
142. Sokal, N.O., Sokal, A.D.: Class E—a new class of high-efficiency tuned single-ended switching power amplifiers. IEEE Journal of Solid-State Circuits **10**, 168–176 (1975)
143. Sokal, N.O., Sokal, A.D.: High-efficiency tuned switching power amplifier. US Patent 3,919,656, 1975
144. Sokal, N.O., Sokal, A.D.: Class E high-efficiency switching-mode tuned power amplifier with only one inductor and one capacitor in load network-approximate analysis. IEEE Journal of Solid-State Circuits **16**, 380–384 (1981)
145. Soma, M., Galbraith, D.C., White, R.L.: Radio-frequency coils in implantable devices: Misalignment analysis and design procedure. IEEE Transactions on Biomedical Engineering **34**, 276–282 (1987)
146. Stuchly, M.A., Stuchly, S.S.: Experimental radiowave and microwave dosimetry. In: Polk, C., Postow, E. (eds.) Handbook of Biological Effects of Electromagnetic Fields, 2nd edn. chap. 8, pp. 295–336. CRC Press, Boca Raton (1996). ISBN 0-8493-0641-8
147. Sullivan, C.R.: Optimal choice for number of strands in a Litz-wire transformer winding. IEEE Transactions on Power Electronics **14**, 283–291 (1999)
148. Tenforde, T.S.: Interaction of ELF magnetic fields with living systems. In: Polk, C., Postow, E. (eds.) Handbook of Biological Effects of Electromagnetic Fields, 2nd edn. chap. 4, pp. 185–230. CRC Press, Boca Raton (1996). ISBN 0-8493-0641-8
149. The MathWorks, Inc.: MATLAB, August, 2006, version 7.3.0.298
150. Troyk, P.R., DeMichele, G.A.: Inductively-coupled power and data link for neural prostheses using a class-e oscillator and fsk modulation. In: 25th Annual International Conference of the IEEE Engineering in Medicine and Biology Society, Cancun, Mexico, September 17–21, 2003, pp. 3376–3379
151. Troyk, P.R., Schwan, A.K.: Closed-loop class E transcutaneous power and data link for MicroImplants. IEEE Transactions on Biomedical Engineering **39**(6), 589–599 (1992)
152. Turgis, D., Puers, R.: Image compression in video radio transmission for capsule endoscopy. Sensors and Actuators A: Physical **123–124**, 129–136 (2005)
153. Utsuyama, N., Yamaguchi, H., Obara, S., Tanaka, H., Fukutaand, S., Nakahira, J., Tanabe, S., Bando, E., Miyamoto, H.: Telemetry of human electrocardiograms in aerial and aquatic environments. IEEE Transactions on Biomedical Engineering **35**, 881–884 (1988)
154. Van Craenenbroeck, T., Vermogenelektronica. Course text H227, K.U. Leuven (2001)
155. Van de Capelle, A.: Informatie-overdracht, deel 1. Vlaamse Technische Kring v.z.w., Leuven (1998)
156. Vandewalle, J.: Systeemtheorie en Regeltechniek, deel 1. Vlaamse Technische Kring v.z.w., Leuven (1999)
157. Van Ham, J., Claes, W., De Cooman, M., Puers, R., Naert, I., Beckers, L., Van Lierde, C.: An autonomous smart dental prosthesis for fast rehabilitation. In: International Workshop on Wearable and Implantable Body Sensor Networks, Boston, U.S., April 3–5, 2006, pp. 100–103. ISBN 0-7695-2547-4
158. Van Ham, J., Naert, I.E., Puers, R.: Design and packaging of a fully autonomous medical monitoring system for dental applications. IEEE Transactions on Circuits and Systems **54**, 200–208 (2007)
159. Van Ham, J., Reynders-Frederix, P., Puers, R.: An autonomous implantable distraction nail controlled by an inductive power and data link. In: TRANSDUCERS'07 and Eurosensors XXI, Lyon, France, June 10–14, 2007, pp. 427–430

160. Van Overstraeten, R., Heremans, P.: Semiconductor Devices. Acco, Leuven, Belgium (1999). ISBN 90 334 3270 6
161. Van Schuylenbergh, K.: Optimization of inductive powering of small bio-telemetry implants. Ph.D. thesis, K.U. Leuven, Belgium (1998)
162. Van Schuylenbergh, K., Puers, R.: Self-tuning inductive powering for implantable telemetric monitoring systems. Sensors and Actuators A: Physical **52**, 1–7 (1996)
163. Von Arx, J.A., Najafi, K.: On-chip coils with integrated cores for remote inductive powering of integrated microsystems. In: TRANSDUCERS'97, Chicago, U.S., June 16–19, 1997, vol. 2, pp. 999–1002. ISBN 0-7803-3829-4
164. von Maltzahn, W.W., Eggleston, J.L.: Electrosurgical devices. In: Bronzino, J.D. (ed.) The Biomedical Engineering Handbook, chap. 83, pp. 1292–1300. CRC Press, Boca Raton (1995)
165. Waterloo Maple Inc.: Maple, February 2007, version 11.0
166. Wilson, B.S., Finley, C.C., Lawson, D.T., Wolford, R.D., Eddington, D.K., Rabinowitz, W.M.: Better speech recognition with cochlear implants. Nature **352**, 236–238 (1991)
167. Wiltshire, M.C.K., Pendry, J.B., Young, I.R., Larkman, D.J., Gilderdale, D.J., Hajnal, J.V.: Microstructured magnetic materials for RF flux guides in magnetic resonance imaging. Science **291**, 849–851 (2001)
168. Zarlink Semiconductor Inc.: Ottowa, Canada, ZL70101 Medical Implantable RF Transceiver, April 2007
169. Ziaie, B., Rose, S.C., Nardin, M.D., Najafi, K.: A self-oscillating detuning-insensitive class-e transmitter for implantable microsystems. IEEE Transactions on Biomedical Engineering **48**(3), 397–400 (2001)
170. Zierhofer, C.M., Hochmair, E.S.: High-efficiency coupling-insensitive transcutaneous power and data transmission via an inductive link. IEEE Transactions on Biomedical Engineering **37**(7), 716–722 (1990)
171. Zierhofer, C.M., Hochmair, E.S.: Geometric approach for coupling enhancement of magnetically coupled coils. IEEE Transactions on Biomedical Engineering **43**, 708–714 (1996)
172. Zulinski, R., Steadman, J.: Class E power amplifiers and frequency multipliers with finite DC-feed inductance. IEEE Transactions on Circuits and Systems **34**, 1074–1087 (1987)

Index

B. Lenaerts, R. Puers, *Omnidirectional Inductive Powering for Biomedical Implants*,